water

MDPI

Article

Synthetic and Natural Surfactants for Potential Application in Mobilization of Organic Contaminants: Characterization and Batch Study

Neda Amanat [1,*], Berardino Barbati [1], Marta M. Rossi [1], Marco Bellagamba [2], Marco Buccolini [2], Luciano Galantini [1] and Marco Petrangeli Papini [1]

[1] Department of Chemistry, Sapienza University of Rome, P.le Aldo Moro 5, 00185 Rome, Italy; berardino.barbati@uniroma1.it (B.B.); martamaria.rossi@uniroma1.it (M.M.R.); luciano.galantini@uniroma1.it (L.G.); marco.petrangelipapini@uniroma1.it (M.P.P.)
[2] Chimec SpA, Via Ardeatina, 00071 Pomezia, Italy; mbellagamba@chimec.it (M.B.); mbuccolini@chimec.it (M.B.)
* Correspondence: neda.amanat@uniroma1.it

Abstract: In this paper, we investigated the abilities of five sugar-based synthetic surfactants and biosurfactants from three different families (i.e., alkyl polyglycoside (APG), sophorolipid (SL), and rhamnolipid (RL)) to dissolve and mobilize non-aqueous phase liquid (NAPL) components, i.e., toluene and perchloroethylene (PCE), adsorbed on porous matrices. The objective of this study was to establish a benchmark for the selection of suitable surfactants for the flushing aquifer remediation technique. The study involved a physicochemical characterization of the surfactants to determine the critical micelle concentration (CMCs) and interfacial properties. Subsequently, a batch study, through the construction of adsorption isotherms, made it possible to evaluate the surfactants' capacities in contaminant mobilization via the reduction of their adsorptions onto a reference adsorbent material, a pine wood biochar (PWB). The results indicate that a synthetic surfactant from the APG family with a long fatty acid chain and a di-rhamnolipid biosurfactant with a shorter hydrophobic group offered the highest efficiency values; they reduced water surface tension by up to 54.7% and 52%, respectively. These two surfactants had very low critical micelle concentrations (CMCs), 0.0071 wt% and 0.0173 wt%, respectively; this is critical from an economical point of view. The batch experiments showed that these two surfactants, at concentrations just five times their CMCs, were able to reduce the adsorption of toluene on PWB by up to 74% and 65%, and of PCE with APG and RL by up to 65% and 86%, respectively. In general, these results clearly suggest the possibility of using these two surfactants in surfactant-enhanced aquifer remediation technology.

Keywords: surfactants; biosurfactant; critical micelle concentration; mobilization; non-aqueous phase liquids

Citation: Amanat, N.; Barbati, B.; Rossi, M.M.; Bellagamba, M.; Buccolini, M.; Galantini, L.; Petrangeli Papini, M. Synthetic and Natural Surfactants for Potential Application in Mobilization of Organic Contaminants: Characterization and Batch Study. *Water* **2022**, *14*, 1182. https://doi.org/10.3390/w14081182

Academic Editor: Laura Bulgariu

Received: 6 March 2022
Accepted: 5 April 2022
Published: 7 April 2022

1. Introduction

Non-aqueous phase liquids (NAPLs), such as petroleum hydrocarbons and chlorinated solvents, are among the most widespread (and consequential) soil and groundwater contaminants, and they are increasingly being recognized as serious environmental problems [1–3]. These water-immiscible organic liquids are classified into light NAPL (LNAPL) and dense NAPL (DNAPL) based on their densities [4]. They are characterized by low water solubility, high hydrophobicity, and a high tendency to accumulate in the soil organic fraction [5,6]. After a spill, NAPLs migrate downward through the vadose zone and remain trapped in the pore space at residual saturation by capillary forces, in the form of separate phase droplets or ganglia [7]. Light NAPLs float at the water table, while DNAPLs can penetrate the water table and migrate downward into the low permeability layer [8,9]. Over time, NAPLs trapped in the interstitial space may slowly dissolve in groundwater,

resulting in long-term persistent sources of aquifer contamination [4]. Due to the unique chemical–physical characteristics of NAPLs, it is particularly difficult to understand and predict their distributions in soils and subsoils, which is an essential basis for determining a proper remediation strategy. Furthermore, conventional remediation technologies, such as pump-and-treat (P&T), have shown severe limitations in recovering these contaminants [10]. P&T is the oldest and the most widely used method for remediation of NAPL contaminations, which often results in low removal efficiency (60%≥) due to a trapped immobile separated phase, low solubility, and high interfacial tension of contaminants with water [11,12]. In this regard, the addition of surfactants has been shown in many studies to significantly increase the recovery of NAPL in less time and at a lower cost by washing/flushing or other remediation technologies [13,14].

Surfactants are amphiphilic organic molecules, typically with a hydrophobic tail group and a hydrophilic head group [15]. They can concentrate at the interface between two immiscible phases, orienting the hydrophobic group toward the organic phase and the hydrophilic group toward the aqueous phase, resulting in a decrease in the interfacial tension (IFT) between the phases [16]. In this way, surfactants can reduce the interfacial tension between NAPL and water and the attractive force between NAPL and soil [17]; thus, improving the displacement and mobility of entrapped NAPL by emulsification. When the surfactant concentration is equal to or greater than the critical micelle concentration (CMC), the monomers spontaneously aggregate into micelles, with the polar head groups exposed to the aqueous phase and the hydrophobic tail groups confined into the core [18], providing a favorable environment for the dispersion of organic compounds [19]. Therefore, micellization can enhance the solubilization of NAPLs from residual trapped ganglia and/or adsorbed phases [20,21]. The CMC is the total surfactant concentration at which the physicochemical property of the system (i.e., surface or interfacial tension) varies the most, and above which, it becomes independent of the surfactant concentration [22,23]. Under the same conditions (e.g., temperature, pressure, pH, ionic strength), micellization strongly depends on the structural molecular properties of the surfactant, such as the size of the head group, length of the alkyl chain, presence of branches, unsaturation, and/or polar groups. Several authors have shown that the CMC decreases with the increasing in alkyl chain length, while it increases in the presence of branching, unsaturation, and/or polar groups. Moreover, the CMC increases with the increasing size of the hydrophilic group, which is mainly due to steric hindrance [18,24–27]. Generally, surfactants are divided into ionic (cationic or anionic), nonionic, or zwitterionic surfactants based on the charge of their polar head group [28]. Many studies have shown that nonionic surfactants are preferable to ionic surfactants in soil remediation [29], due to the adsorption of cationic surfactants [29] or precipitation of anionic surfactants [30] with some counterions. It has been demonstrated that nonionic surfactants, since the hydrophilic group has no charge, have negligible interactions with soil particles [31,32] and offer better solubilization and economic advantages. Moreover, surfactants can be classified into synthetic and natural surfactants according to their production methods, which are obtained by chemical synthesis and microbial secondary metabolism, respectively [33,34]. However, the use of synthetic surfactants as extractive agents in soils remains a problem because, on the one hand, they are derived from fossil raw materials [19], and, on the other hand, they tend to remain partially in the soil due to their toxicity and low biodegradability [35]. Recently, researchers have focused on surfactants that are 100% bio-based [36], such as sugar-based nonionic surfactants derived from renewable sources (e.g., biomass containing sugars and fatty acid esters) [26].

Considering the use of surfactants in the context of environmental remediation, this study focused on two subclasses of bio-based surfactants, alkyl polyglycosides (APGs), which are the products of a catalyzed chemical reaction of glucose-derived raw materials with fatty alcohol, and rhamnolipids and sophorolipids, which are biologically produced, mainly by the bacterium *Pseudomonas aeruginosa* and the yeast of the genus Candida, particularly *C. bombicola* and *C. apicola*, respectively. Literature studies show that APGs,

rhamnolipids, and sophorolipids are good candidates as solubilizers and emulsifiers for soil and aquifer remediation and enhanced oil recovery [37,38]. In addition, rhamnolipids and sophorolipids have the positive aspect of promoting biodegradation of organic compounds during remediation [39,40]. Overall, this research aimed to provide a benchmark for the identification and characterization of potential surfactants for in-situ flushing of contaminated sites. In this regard, we investigated the abilities of five nonionic and biodegradable surfactants to solubilize and mobilize NAPL components adsorbed to a porous medium. The study initially involved the chemical–physical characterizations of surfactants to determine their CMCs and surface behavior parameters by measuring the liquid–air surface tension at different surfactant concentrations. In the second phase, a study on the mobilization of the adsorbed pollutants was carried out. This involved adsorption isotherm batch studies to determine the effectiveness of the surfactants in enhancing the mobilization of NAPLs by reducing their adsorption on a porous reference material.

2. Materials and Methods

This study began with the characterization of critical micelle concentrations (CMCs) of distinctive types of nonionic surfactants, both synthetic and biosurfactants; then an experimental setup was used to study the efficiencies of the surfactants to mobilize organic contaminants, in batch mode operation.

2.1. Materials

2.1.1. Synthetic and Biological Surfactants

Five different surfactants were used in this study, representing different families, including two synthetic surfactants from the alkyl polyglycolide family (APG1 and APG2) and three biosurfactants, one from the sophorolipid family (SL) and two from the rhamnolipid family (RL1 and RL2). The general APG structure is shown in Figure 1a. Its hydrophilic moiety consists of oligomeric glycosidic units (mono-, di-, tri-, or more) obtained from starch, corn, wheat, or potato, and also from monomeric carbohydrates. For the lipophilic part, fatty alcohol blends were used [41]. APG blends were provided, which differed mainly in the lengths of the fatty acid chains (i.e., shorter for APG1 than for APG2). A lower polymerization degree of the polysaccharide block is also shown by APG2.

The sophorolipid, whose solution is hereinafter referred to as SL, comprises a hydrophilic moiety consisting of sophorose, a 1,2 disaccharide of glucose, and a lipophilic part consisting of a fatty acid chain. The fatty acid may have one or more unsaturations and is usually 16 or 18 C atoms long. The fatty acid carboxylic group may be free or involved in a lactonic bond, usually with the C4 hydroxy group of a glucose unit (Figure 1b,c). The molecule can be non-, mono-, or di-acetylated at the glucose rings [42].

The rhamnolipids, whose molecular structures are reported in Figure 1d,e, are classified according to the number of rhamnoses (one/mono or two/di), fatty acid residues (one or two), and fatty acid compositions. The length of the constituent fatty acids and their combinations are largely variable, although mono-rhamnolipid (Figure 1e) and di-rhamnolipid (Figure 1d) are typically the dominant components in a naturally produced mixture [42]. Two types of rhamnolipids were tested, differing in their physical states, a water solution rhamnolipid (RL1) and a powder one dissolved in water (RL2).

It should be mentioned that the biosurfactants used in this work were raw mixtures obtained via secondary metabolism without any separation processes.

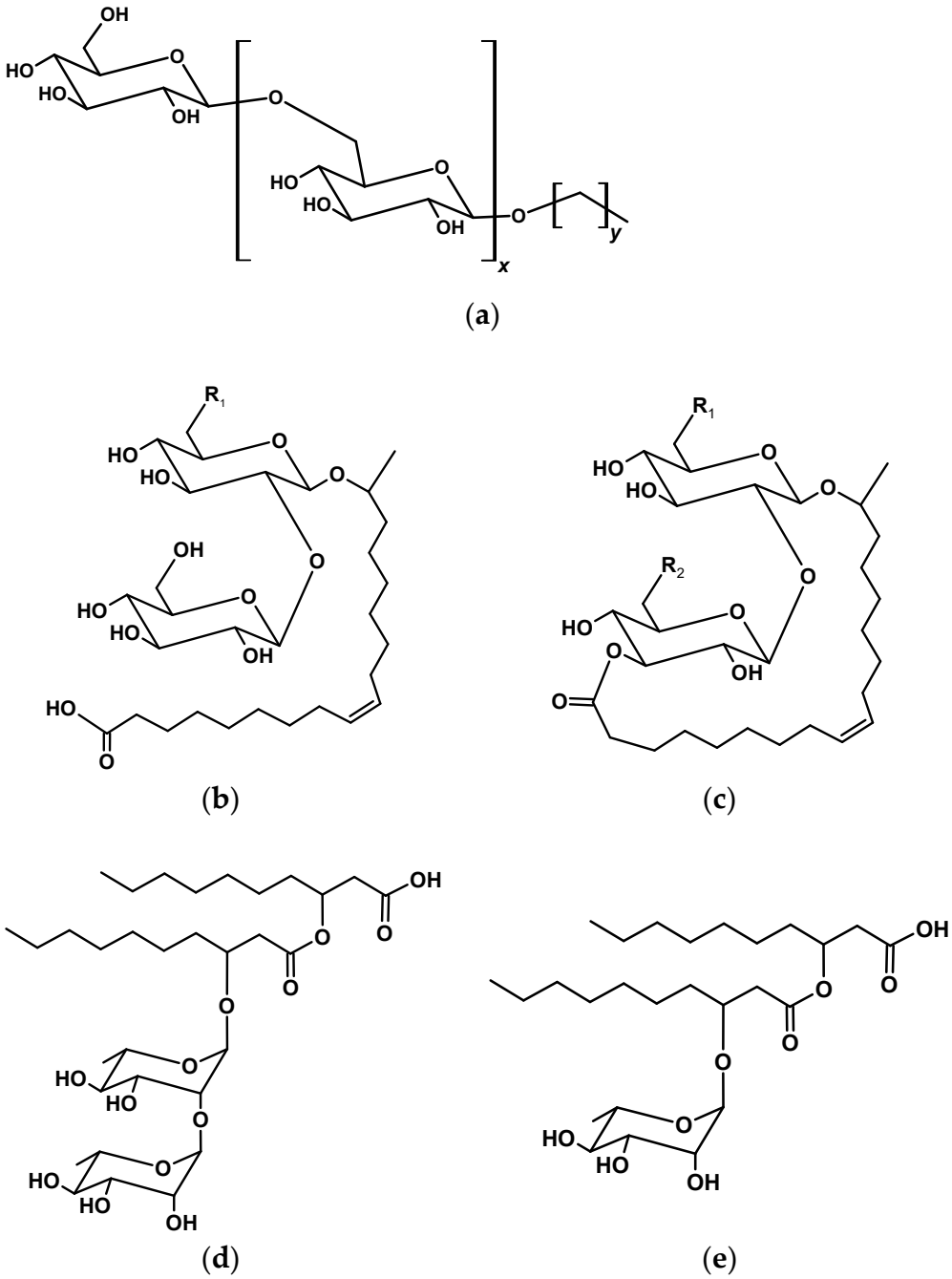

Figure 1. The general structures of surfactants used in this study. (**a**) Alkyl polyglycoside; (**b**) sophorolipid open structure; (**c**) sophorolipid lactonic structure; R_1 and R_2 groups can be a hydroxyl or acetate group (OH or OAc); (**d**) di-rhamnolipid; (**e**) mono-rhamnolipid.

2.1.2. Pine Wood Biochar

Pine wood biochar (PWB) was used as sorbent reference material for batch tests. PWB was obtained from the gasification of wood at approximately 850 °C in V 3.90 Burkhardt and ECO 180 HG wood gas generator (Burkhardt GmbH, Plößberg bei Tirschenreuth, Germany). This microporous material, with a total pore volume of 0.383 $cm^3\ g^{-1}$, has a high specific surface area (343 ± 2 $m^2\ g^{-1}$) and a high carbon content (95.84 wt%) [43]. The large adsorption capacity of this material for organic contaminants was demonstrated in previous studies [43,44].

2.2. Critical Micelle Concentration (CMC) Measurement

This study was initiated with the characterization of the selected surfactants by determining their critical micelle concentrations (CMCs). A series of surface tension measurements of the surfactants were performed, as functions of the concentrations, according to the ring detachment method, by a MWG LAUDA tensiometer (Lauda-Königshofen, Germany), using a platinum-iridium alloy ring with a diameter of 0.95 cm [45,46]. During the experiment, each surfactant solution was diluted with high purity milli-Q water, and the concentration gradually decreased, starting from 1 wt% in steps of 0.2 wt%. Since the surface tension measurement is sensitive to impurities [47], the ring was carefully heated with a flame before each measurement and the sample holder was cleaned first with distilled water, then with nitric acid, and finally with ultrapure milli-Q water. To calculate the CMC value, the surface tension vs. the logarithm of the surfactant concentration was reported. The data were fitted with two linear regressions, one below the CMC where surface tension decreases with increasing concentrations and the other above the CMC where the surface tension remains constant, and the CMC values were calculated from the breakpoints of the two regions.

2.3. Batch Configuration

A thermodynamic study (adsorption isotherm) was performed to assess the mobilization capacity of surfactants by evaluating the reduction in adsorption capacity of contaminants on a reference sorbent material in the presence of surfactants. Two organic compounds were selected as target contaminants, toluene and tetrachloroethylene (PCE), representative of LNAPL and DNAPL constituents, respectively. To achieve a maximum adsorption condition, far superior to any soil, the carbonaceous reference sorbent material pine wood biochar (PWB, Plößberg bei Tirschenreuth, Germany) was selected. Previous studies have shown that this material has a high adsorption capacity due to its high organic carbon content and remarkable surface development, making it an alternative to activated carbon [48,49]. A series of isothermal batch experiments with PWB/contaminant/surfactant were conducted at room temperature (23 $\pm$ 2 °C) and pressure in 20 mL batch reactors (VWR International glass vials, Milan, Italy), using different amounts of sorbent material (10, 20, 50, 80, 100, and 200 mg), and 50 mg L^{-1} of contaminant solution. The contaminated solutions were prepared in distilled water and stored in gas-tight collapsible Tedral bags® (Supelco, Bellefonte, PA, USA), which prevent the formation of headspace and ensure constant maintenance of the concentration of the solution containing volatile compounds [50].

Different concentrations of each surfactant were investigated, below the critical micelle concentration (0.5 $\times$ CMC), at five times the CMC (5 $\times$ CMC), and far above the CMC (5% (v/v)). For the experiments at the highest surfactant concentrations (5% (v/v)), the ratios between the weight percent concentrations of the used surfactant solution and the solutions at CMC are reported in Table 1.

Table 1. Ratios among the effective concentrations of the five surfactants at 5% (v/v) and CMC.

Material	APG1	APG2	SL	RL1	RL2
$C_{5\%(v/v)}$/CMC	13	90	19	169	15

Reference tests were performed under the same operating conditions but without surfactant solutions. Samples of PWB and the contaminants in the presence and in the absence of surfactants were prepared in glass vials. The glass vials were filled without creating headspace, to avoid dispersion of contaminants in the gas phase of each glass reactor, hermetically sealed with a Teflon face gray butyl stopper (Wheaton, Millville, NJ, USA), crimped by an aluminum cap, and stirred on rotating plates for 24 h. Each test was performed in duplicate to evaluate reproducibility. The initial concentration of the contaminant was analyzed at time zero (C_0) and after 24 h (C_e). This is the time required to

reach the thermodynamic equilibrium condition [43] between the sorbed and the dissolved contaminant in the liquid phase.

2.4. Analytical Methods

The contaminants toluene and PCE were determined using a Dani master gas chromatograph (GC) equipped with a flame ionization detector (FID) and a TRB624 capillary column (30 m × 0.53 mm ID × 3 um), with an HSS Dani 86.50 headspace auto-sampler (Dani Instrument, Contone, Switzerland). The samples were placed in the auto-sampler carousel, first passed in a thermostatic oven at 80 °C for 1 min. Then the gas phase was injected into the chromatographic column for analysis. Helium (He) was used as the carrier gas at a flow rate of 10 mL min^{-1}, the injection temperature was set at 180 °C, and the FID temperature at 300 °C. The analysis was performed with a temperature ramp, at first at 60 °C for 3 min with a gradient of 30 °C min^{-1} and the second ramp was at 120 °C for 1 min [43].

2.5. Calculations

To compare the performance of the different surfactants, the efficiency and effectiveness parameters were evaluated both for the adsorption to the liquid–air surface and for the reduction of surface tension. In this regard, the following parameters were calculated:

The Gibbs adsorption isotherm equation (Equation (1)) was used to calculate the maximum (saturated) surface excess concentration.

$$\Gamma_{max} = -\frac{1}{2.303nRT}\left(\frac{\partial\gamma}{\partial \log C}\right) \quad (1)$$

where Γ_{max} is the maximum excess surface concentration (mol cm^{-2}), n is the number of the solute species, which, for the nonionic surfactant, is equal to 1, R is the gas constant value (8.314 J/mol K), T is the ambient temperature (K), and $\left(\frac{\partial\gamma}{\partial \log C}\right)$ is the slope of the linear fit of the data below the CMC.

The surface efficiency at the CMC was calculated according to Equation (2),

$$\pi_{CMC} = \gamma_0 - \gamma_{CMC} \quad (2)$$

where γ_0 and γ_{CMC} are the surface tensions of the pure solvent (water) and surfactant solution at CMC, respectively.

The efficiency of adsorption of the surfactant or the surface tension reduction efficiency (pC_{20}) was defined as the negative logarithm of the surfactant concentration needed for reduction of the surface tension of water by 20 mN m^{-1} (C_{20}).

$$pC_{20} = -\log C_{20} \quad (3)$$

Furthermore, a thermodynamic study (adsorption isotherm) was conducted to investigate the capacity of different types of surfactants to reduce the adsorption of the contaminant on the sorbent material. The Langmuir isotherm model was used for equilibrium data fitting purposes. The equation is reported in Equation (4).

$$q_e = q_{max}\frac{K_L C_e}{1 + K_L C_e} \quad (4)$$

where q_{max} (mg g^{-1}) is the maximum quantity of the adsorbed species, K_L is the Langmuir thermodynamic constant (L mg^{-1}), and C_e is equilibrium concentration (mg L^{-1}). Parameter optimizations were obtained by the nonlinear regression method available in Sigma Plot 12.

3. Results and Discussion

3.1. Critical Micelle Concentration (CMC) Determination

The plots of the surface tension vs. log of concentration are reported in Figure 2a,b for the aqueous solutions of the surfactants (i.e., APG1, APG2, SL, RL1, and RL2), showing the typical pattern with two slopes, whose intersection provides the CMC values. These values are listed in Table 2, along with the surface tension value at CMC (γ_{CMC}), maximum surface excess concentration (Γ_m), surfactant effectiveness (π_{CMC}), adsorption efficiency (pC_{20}), and the derived CMC/C_{20} parameter.

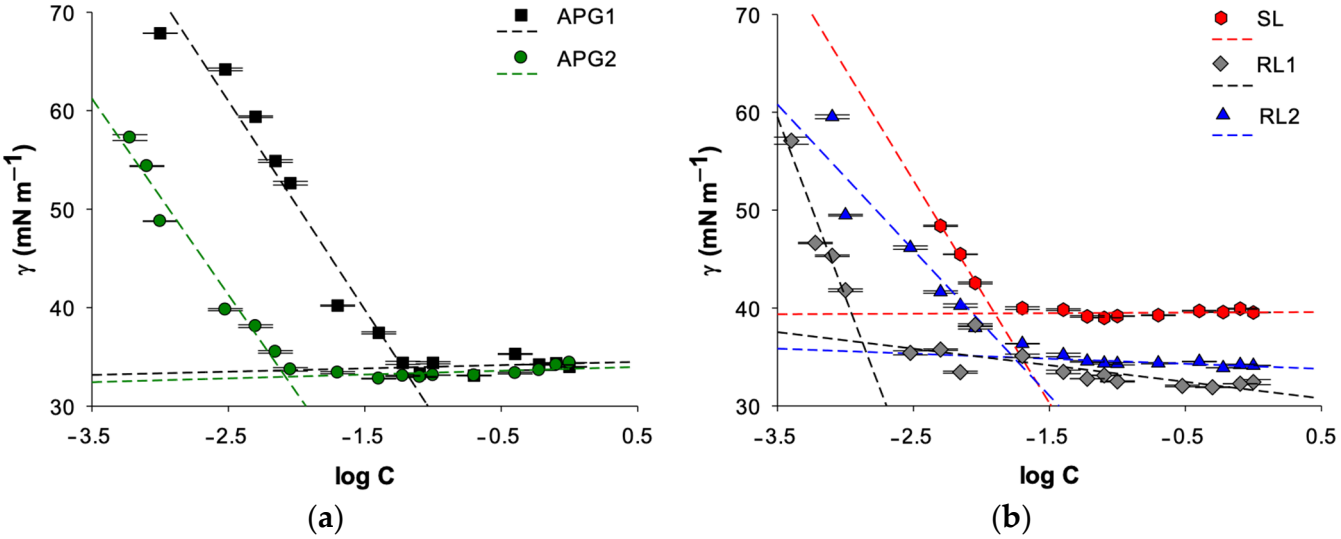

Figure 2. Surface tension vs. log of surfactant concentration for (**a**) synthetic surfactants (APG1 and APG2: alkyl polyglycosides); (**b**) biosurfactants (SL: sophorolipid, RL1 and RL2: rhamnolipids).

Table 2. Micellar and surface properties of surfactants aqueous solutions at 298.15 K and atmospheric pressure.

Surfactant	γ_{CMC} (mN/m)	CMC (wt%)	$\Gamma_{max} \times 10^{10}$ (mol/cm^2)	π_{CMC} (mN/m)	pC_{20}	CMC/C_{20}
APG1	39.925	0.0601	3.711	38.875	2.113	7.799
APG2	32.954	0.0071	4.212	39.846	2.978	6.704
SL	39.451	0.0125	3.983	33.348	2.489	3.870
RL1	36.450	0.0013	6.446	36.349	3.317	2.785
RL2	34.945	0.0173	2.606	37.855	2.963	15.907

An inspection of the table shows ranges for the values of CMC ($10^{-3} \div 6 \times 10^{-2}$ wt%), γ_{CMC} (32.9 ÷ 39.9 mN m^{-1}), π_{CMC} (32.8 ÷ 39.8 mN m^{-1}), Γ_m ($2.6 \times 10^{10} \div 4.2 \times 10^{10}$ mol cm^{-2}), pC_{20} (2.1 ÷ 3.3), and CMC/C_{20} ratio (2.7 ÷ 15.9) in agreement with those expected for nonionic sugar-based surfactants (CMC = $11 \times 10^{-4} \div 6$ %wt, γ_{CMC} = 29 ÷ 45 mN m^{-1}, π_{CMC} = 27 ÷ 44 mN m^{-1}, $\Gamma_m = 1.2 \times 10^{10}$–$13 \times 10^{11}$ mol cm^{-1}, pC_{20} = 1.5 ÷ 6 and CMC/C_{20} = 3.9 ÷ 27) [18,23,26,51–56].

In detail, one should notice that the synthetic APG1 has the highest CMC (6×10^{-2} wt%), whereas a much smaller value is measured for APG2 (7×10^{-3} wt%). The comparisons between the APG surfactants show that APG2 has higher values for pC_{20} (2.978), Γ_m (4.212 mol cm^{-3}), and surfactant efficiency (39.846 mN m^{-1}) than APG1 (pC_{20} = 2.113, Γ_m = 3.711 mol cm^{-3}, and surfactant efficiency of 39.846 mN m^{-1}). Interestingly, the efficiency of APG2 is the largest compared to the whole set of the investigated surfactants. The observed behavior can be ascribed to the longer alkyl chain and the shorter polysaccharide block of APG2 compared to those of APG1.

For SL, an intermediate CMC value (0.0125 wt%) was detected; it is noteworthy that both γ_{CMC} and CMC were consistent with the ranges reported in the literature for sophorolipids (11×10^{-4}–25×10^{-3} wt%) [51]. In addition, this material showed the lowest surface tension reduction efficiency (33.348 mN m^{-1}) among all five materials. Indeed, for this material, it was hypothesized that its mixture contained a greater proportion of acidic forms than lactonic ones since lactonic sophorolipids are always characterized by a better surface activity and a lower CMC [57]. The surface properties of SL can be attributed to molecular features. A general high hydrophobicity is provided by the presence of a large number of carbon atoms ($C \geq 20$). In addition, specific effects are imparted by a carbon–carbon double bond, a hydrophilic group in a non-terminal position (i.e., with a CH_3 group acting as a branch), and a carboxylic group sufficiently distant for cyclization, which determine low values of the pC_{20} factor and Γ [26,27].

Furthermore, the results show that RL1 has the lowest CMC (1.34×10^{-3} wt%), which is remarkably lower than the one estimated for RL2 (1.73×10^{-2}). In any case, both CMC values are within the range reported in the literature for rhamnolipids (0.001–0.2 wt%) [23,55]. It was also found that RL2 is more effective at lowering the surface tension of the solution than RL1, which has a lower π_{CMC} (36.349 mN m^{-1}) [24,58,59]. In general, based on physicochemical parameters, it can be assumed that RL1 consists mainly of mono-rhamnolipids with long alky chains. These properties guarantee the low CMC and high values of pC_{20} and Γ. Additionally, the very low value of the CMC/C_{20} ratio (2.785) signifies an excessive tendency of RL1 to micellization rather than surface adsorption [27], justifying the lower surfactant effectiveness value for this material compared to RL2. In contrast, RL2 might be predominantly a di-rhamnolipid with a shorter hydrophobic group, based on the higher CMC, lower value of pC_{20}, and significantly lower value of Γ_m [24]. Further, the very high CMC/C_{20} ratio (15.907) of RL2 indicates a greater tendency for this material to adsorb and orient on the surface, as it was found to be more effective than RL1 in reducing surface tension.

3.2. Batch Tests

3.2.1. Adsorption Isotherm Study in the Presence of Toluene as a Contaminant

The adsorption isotherm tests were carried out to evaluate the mobilization capacity of the five surfactants (APG1, APG2, SL, RL1, and RL2) in the presence of different families of organic pollutants, i.e., toluene from the BTEX group and PCE representing the chlorinated solvent family, by evaluating the surfactant induced reduction of adsorption capacity on PWB. Figure 3 reports the adsorption isotherms of toluene on PWB in the absence (Reference) and the presence of surfactant solutions below (i.e., 0.5 × CMC) and above their CMC (i.e., 5 × CMC and 5% (v/v)). We should mention that a lower CMC is important from an economical point of view, where less surfactant is required to effectively solubilize contaminants. The experimental data were always well-represented by the Langmuir adsorption isotherm (Figure 3). The Langmuir isotherm was used with the sole purpose of comparing the results obtained in the various experimental conditions; the adsorption data showed a plateau trend that could be well-fitted by this model. This is also confirmed by the high regression coefficient R2 for each surfactant at different concentrations, as reported in Table 3. As it can be seen in Figure 3 and Table 3, the adsorption capacity of toluene on PWB decreased remarkably in the presence of the surfactants, except for RL2 at low concentrations. In general, the results indicate that the presence of the surfactant leads to a decrease in adsorption on PWB as a function of the concentration. This can be explained by the effect of the surfactant, which enhances the apparent solubility of the hydrophobic compound; that is, the "driving forces" for the desorption of the sorbed compounds in the liquid phase. At the same time, it was also observed that in the presence of the surfactant, the KL value decreased with the increasing surfactant concentration, indicating a decrease in the affinity of toluene for PWB. Indeed, for synthetic surfactants (i.e., APG1 and APG2) the maximum adsorption (q_{max}), with respect to the maximum adsorption of toluene on PWB (reference test, 77.71 ± 2.5 mg g^{-1}), dropped off with surfactant concentration,

providing adsorption reductions at 0.5 × CMC, 5 × CMC and 5% (v/v) of 53%, 73%, and 78% for APG1 and 62%, 74%, and 82% for APG2, respectively. In parallel, a smoother increasing trend in the adsorption reduction was measured in the case of the biomaterials SL (57%, 60%, and 61%) and RL2 (64%, 65%, and 69%). A less continuous variation was shown by RL1, for which an adsorption reduction much lower than for the other surfactants was measured at the low concentrations of 0.5 × CMC and 5 × CMC (about 34% for both concentrations); a jump to 71% was revealed at 5% (v/v), equal to 169 times of CMC. Interestingly, these results confirm those obtained from the characterization of CMC, where RL1 was less efficient compared to the other materials.

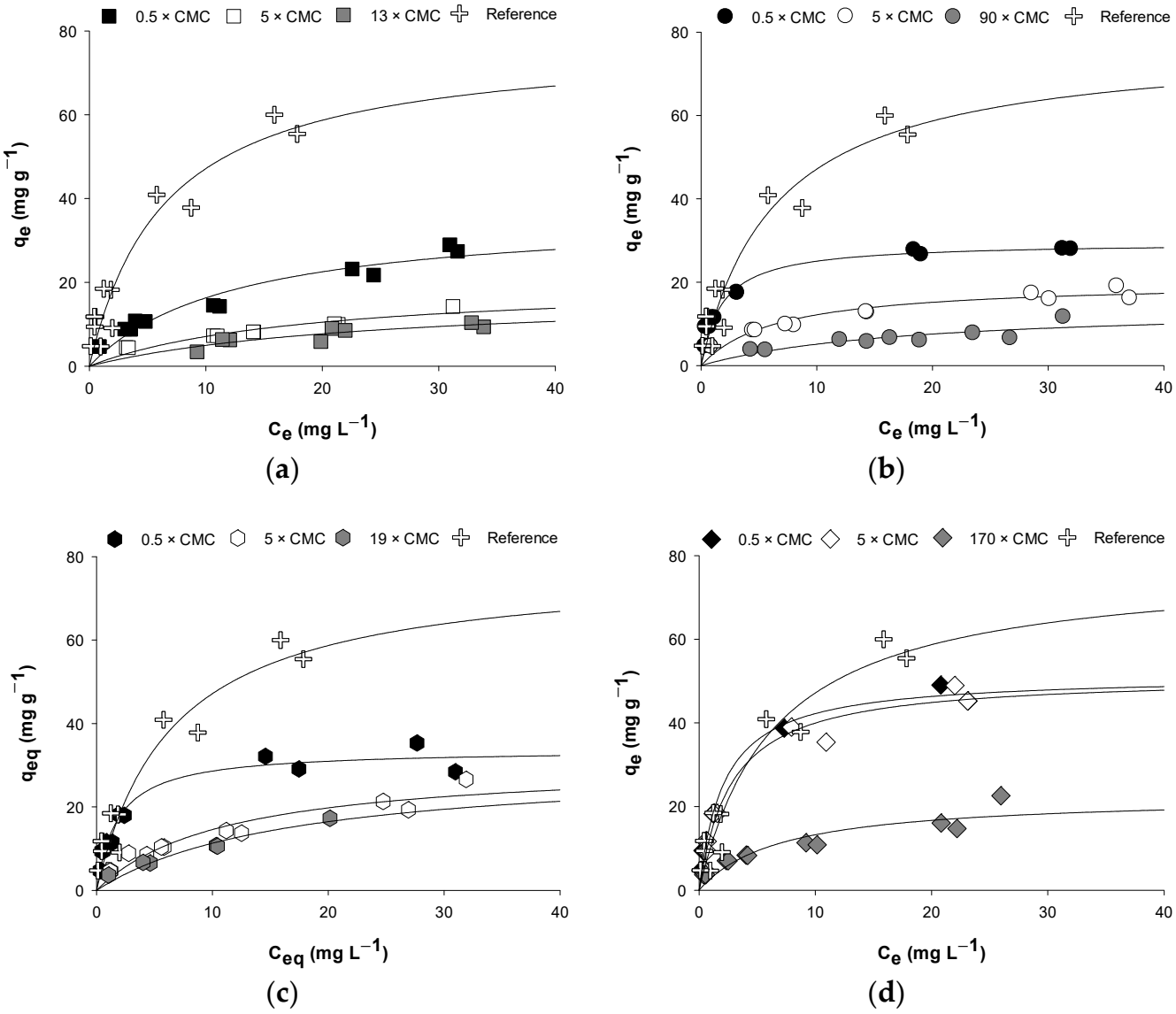

Figure 3. *Cont.*

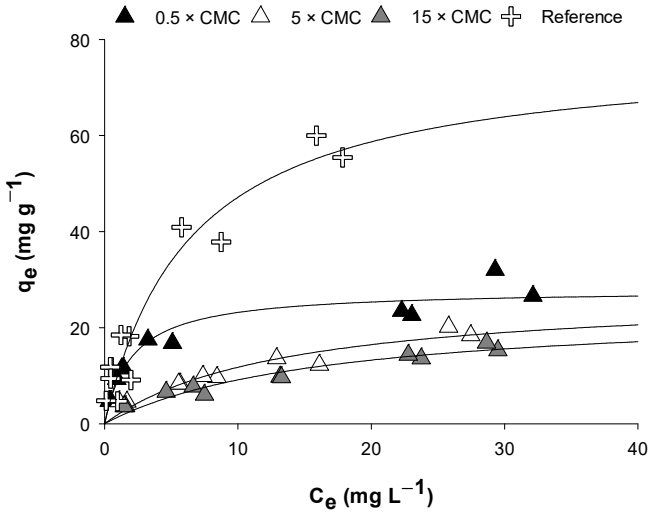

(**e**)

Figure 3. Isotherm curve of the adsorption of toluene on PWB in surfactant solutions at different concentrations for (**a**) APG1, (**b**) APG2, (**c**) SL, (**d**) RL1, and (**e**) RL2.

Table 3. Optimized parameters of the Langmuir model of toluene on PWB in the presence and in the absence of surfactants.

		Surfactant Solution Concentration		
Material	**Langmuir Parameters**	**0.5 × CMC**	**5 × CMC**	**5% (*v*/*v*)**
APG1	q_{max} (mg g^{-1})	36.42 ± 3.9	20.28 ± 4.1	17.36 ± 5.3
	K_L (L mg^{-1})	$81 \times 10^{-3} \pm 21 \times 10^{-3}$	$53 \times 10^{-2} \pm 21 \times 10^{-3}$	$40 \times 10^{-3} \pm 23 \times 10^{-3}$
	R^2	0.94	0.89	0.78
APG2	q_{max} (mg g^{-1})	29.58 ± 1.3	20.14 ± 1.4	14.36 ± 4.8
	K_L (L mg^{-1})	$55 \times 10^{-2} \pm 91 \times 10^{-3}$	$15 \times 10^{-2} \pm 36 \times 10^{-3}$	$55 \times 10^{-3} \pm 39 \times 10^{-3}$
	R^2	0.95	0.91	0.98
SL	q_{max} (mg g^{-1})	33.75 ± 1.5	30.77 ± 2.8	30.38 ± 2.6
	K_L (L mg^{-1})	$55 \times 10^{-2} \pm 88 \times 10^{-3}$	$14 \times 10^{-2} \pm 30 \times 10^{-3}$	$19 \times 10^{-2} \pm 70 \times 10^{-3}$
	R^2	0.96	0.94	0.95
RL1	q_{max} (mg g^{-1})	51.31 ± 1.3	51.16 ± 2.5	22.53 ± 3.3
	K_L (L mg^{-1})	$46 \times 10^{-2} \pm 39 \times 10^{-3}$	$36 \times 10^{-2} \pm 56 \times 10^{-3}$	$14 \times 10^{-2} \pm 56 \times 10^{-3}$
	R^2	0.99	0.97	0.84
RL2	q_{max} (mg g^{-1})	27.95 ± 1.5	27.44 ± 4.1	24.05 ± 3.4
	K_L (L mg^{-1})	$48 \times 10^{-2} \pm 98 \times 10^{-3}$	$75 \times 10^{-3} \pm 24 \times 10^{-3}$	$61 \times 10^{-3} \pm 18 \times 10^{-3}$
	R^2	0.93	0.91	0.93
Reference test in the absence of surfactant				
Isotherm Toluene-PWB	q_{max} (mg g^{-1})	77.71 ± 2.5		
	K_L (L mg^{-1})	$15 \times 10^{-2} \pm 55 \times 10^{-3}$		
	R^2	0.97		

3.2.2. Adsorption Isotherm Study in the Presence of Tetrachloroethylene as a Contaminant

This section presents the results of the isothermal study of PCE on PWB in the absence—and in the presence—of the five surfactants, as reported in Figure 4 and Table 4. In this regard, the same isothermal tests were performed, and the curves were fitted by Langmuir's isothermal model. It is noticeable that, for the reference test, in the absence of the surfactant, the adsorption on PWB is much larger for PCE than for toluene, confirming a higher affinity of PWB for PCE compared to toluene. In fact, higher values of q_{max} and KL were calculated for the isotherm of PCE, namely 114 ± 7.8 mg g^{-1} and $29 \times 10^{-2} \pm 48 \times 10^{-3}$ L mg^{-1},

respectively. The lower solubility in water and the higher octanol–water partition coefficient (KOW) of PCE (0.15 g L^{-1} and 3.40, respectively) compared to toluene (0.52 g L^{-1} and 2.73, respectively) confirm the higher hydrophobicity of PCE than toluene, thus explaining the observed adsorption results [60]. The greater adsorption of PCE compared to toluene could also be due to the steric effect limiting the accessibility of toluene in the pores of the sorbent material [61]. Moreover, the same trends were observed in the presence of surfactants and PCE as a contaminant, in which adsorption capacities decrease with the rising concentrations of surfactants. This confirms the affinity of surfactants in mobilization of PCE.

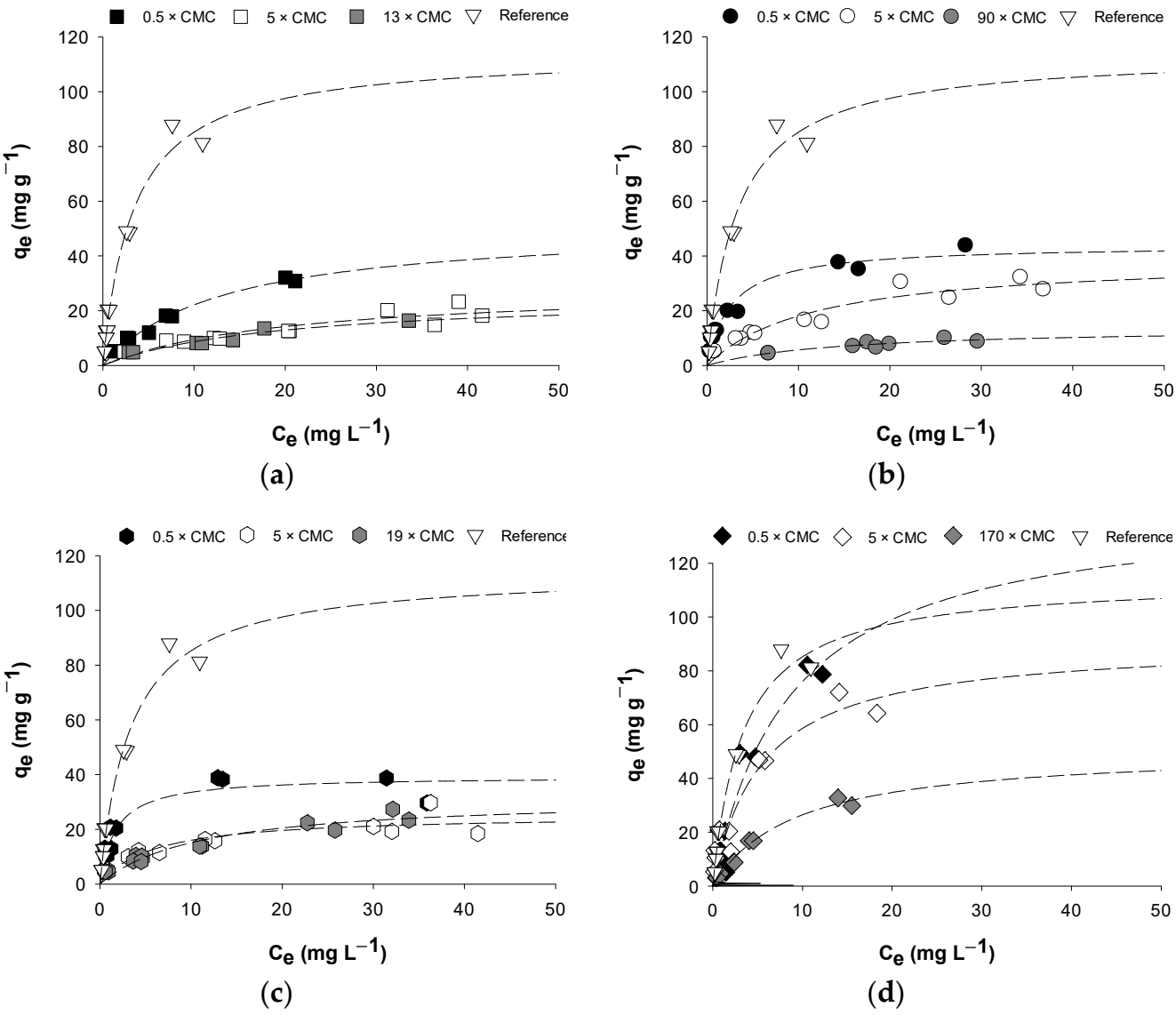

Figure 4. *Cont.*

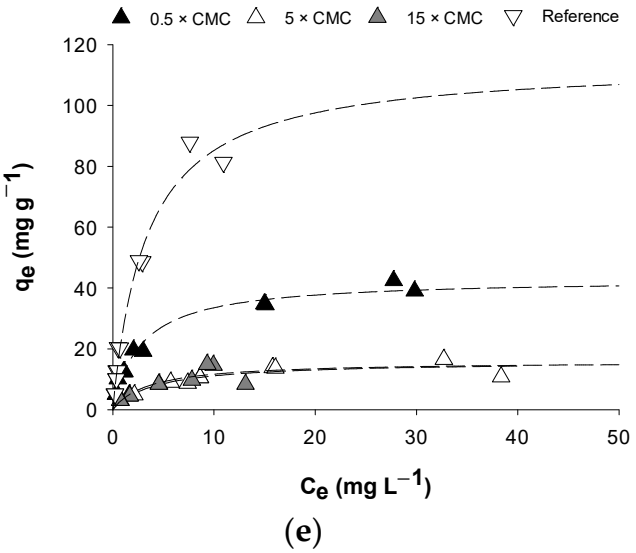

Figure 4. Isotherm curve of PCE on PWB, and surfactant solutions in different concentrations: (**a**) APG1, (**b**) APG2, (**c**) SL, (**d**) RL1, (**e**) RL2.

Table 4. Optimized parameters of the Langmuir model of PCE on PWB in the presence and in the absence of surfactants.

		Surfactant Solution Concentration		
Material	**Langmuir Parameters**	**0.5 × CMC**	**5 × CMC**	**5% (*v*/*v*)**
APG1	q_{max} (mg g^{-1})	51.35 ± 4.1	28.68 ± 5.6	25.55 ± 5.4
	K_L (L mg^{-1})	$76 \times 10^{-2} \pm 12 \times 10^{-3}$	$5 \times 10^{-2} \pm 21 \times 10^{-3}$	$51 \times 10^{-2} \pm 20 \times 10^{-3}$
	R^2	0.98	0.83	0.9153
APG2	q_{max} (mg g^{-1})	44.02 ± 2.5	39.42 ± 4.7	13.90 ± 2.5
	K_L (L mg^{-1})	$38 \times 10^{-2} \pm 68 \times 10^{-3}$	$85 \times 10^{-3} \pm 25 \times 10^{-3}$	$69 \times 10^{-3} \pm 28 \times 10^{-3}$
	R^2	0.96	0.91	0.86
SL	q_{max} (mg g^{-1})	39.32 ± 2.7	31.85 ± 3.3	25.30 ± 2.8
	K_L (L mg^{-1})	$58 \times 10^{-2} \pm 13 \times 10^{-2}$	$17 \times 10^{-2} \pm 28 \times 10^{-3}$	$90 \times 10^{-3} \pm 24 \times 10^{-3}$
	R^2	0.90	0.80	0.92
RL1	q_{max} (mg g^{-1})	142.32 ± 30	90.75 ± 12.6	50.83 ± 4.6
	K_L (L mg^{-1})	$12 \times 10^{-2} \pm 44 \times 10^{-3}$	$18 \times 10^{-2} \pm 62 \times 10^{-3}$	$11 \times 10^{-2} \pm 19 \times 10^{-3}$
	R^2	0.92	0.91	0.98
RL2	q_{max} (mg g^{-1})	43.00 ± 1.66	15.86 ± 1.62	15.87 ± 3.4
	K_L (L mg^{-1})	$35 \times 10^{-2} \pm 49 \times 10^{-3}$	$23 \times 10^{-2} \pm 83 \times 10^{-3}$	$27 \times 10^{-2} \pm 16 \times 10^{-3}$
	R^2	0.98	0.81	0.96
Reference test in the absence of surfactant				
Isotherm PCE-PWB	q_{max} (mg g^{-1})	114.12 ± 7.8		
	K_L (L mg^{-1})	$29 \times 10^{-2} \pm 48 \times 10^{-3}$		
	R^2	0.98		

As shown in Figure 4, surfactants APG1, APG2, SL, and RL2 significantly reduced the adsorption of PCE on PWB, even at concentrations below their CMCs. The percent reductions in the presence of these surfactants at 0.5 × CMC were 55%, 61%, 65%, and 62%, respectively. Above the CMC, q_{max} for APG1, SL, and RL2 decreased further by 74%, 72%, and 86%, respectively. It is worth noting that the reductions were almost the same for the 5 × CMC and 5% (v/v) for these three materials (Figure 4a,c,e). Meanwhile, for the synthetic surfactant APG2, a more evident reduction in adsorption of PCE was observed in the batch system with increasing concentrations (Figure 4b), with a reduction of about 65% calculated for the 5 × CMC, while a reduction of 88% was observed for the 5% (v/v) mixture of the surfactant in water. In contrast, the biosurfactant RL1 showed a dissimilar behavior (Figure 4d). Indeed, this material failed to increase the solubility of PCE below the CMC, with the calculated q_{max} (142.32 ± 30 mg g^{-1}) even higher than in the reference test. This can be due to the formation of hemimicelles onto the surfaces of adsorbent material (i.e., PWB). Hemimicelles are surfactant monomer aggregates with the hydrophilic and hydrophobic moieties oriented toward the aqueous phase and solid surface, respectively. In this way, due to the amphiphilic nature of surfactants, hemimicelles can solubilize and retain hydrophobic compounds [52,62–64]. Although, when the concentration raised above the CMC, the effect of the appearance of biosurfactant RL1 became apparent, reducing the adsorption capacities by 20% and 55% for 5 × CMC and 5% (v/v), respectively. From the data, the biosurfactant RL1 reduced the adsorption least efficiently.

4. Conclusions

We characterized the interfacial properties of five nonionic biodegradable surfactants, in order to preliminary evaluate the capacity of different surfactants for remediation purposes and mobilization of sorbed NAPLs onto soil and aquifer. Then, by an adsorption study, we deeply investigated the effect of the surfactant on the adsorption behavior of PCE and toluene onto a reference adsorbent material (PWB). Overall, the investigated surfactants, i.e., two synthetic surfactants (APG1 and APG2) and three biosurfactants (SL, RL1, and RL2), significantly improved the potential mobilization of both organic target compounds. The results from the CMC characterization indicated that the lowest CMCs among the synthetic surfactants and biosurfactants belonged to APG2 and RL1, 0.0071 wt% and 0.0013 wt%, respectively. Nevertheless, the surfactants APG2 and RL2 offered the highest efficiency values, respectively. Moreover, results from the batch study confirmed the results of the characterization study, as APG2 and RL2 showed the highest abilities to reduce the adsorption of contaminants on the PWB. In general, the results demonstrated the significant capacities of synthetic surfactant APG2 and biosurfactant RL2 in the mobilization of hydrophobic contaminants. Interestingly, these two surfactants at just five times their CMCs reduced maximum adsorption capacities of toluene on PWB to 74% and 65%, and PCE on PWB by up to 65% and 86%, respectively, for APG2 and RL2. In conclusion, the biosurfactant RL2 could be the best candidate for surfactant-enhanced aquifer remediation technology (SEAR) due to the high effectiveness of this material and its low environmental impact, with respect to its natural base. Future research will focus on a column study to simulate the applicability of different surfactants in the in-situ flushing remediation technology.

Author Contributions: Conceptualization, N.A. and M.P.P.; formal analysis, N.A. and M.P.P.; investigation, N.A. and B.B.; resources, M.P.P. and M.B. (Marco Buccolini); data curation, N.A. and M.M.R.; writing—original draft preparation, N.A., B.B., M.B. (Marco Bellagamba); writing—review and editing, N.A., M.M.R., L.G. and M.P.P.; visualization, N.A., L.G. and M.P.P.; supervision, M.B. (Marco Buccolini), L.G. and M.P.P.; project administration, M.P.P. All authors have read and agreed to the published version of the manuscript.

Funding: This research received no external funding.

Institutional Review Board Statement: Not applicable.

Informed Consent Statement: Not applicable.

Data Availability Statement: Not applicable.

Acknowledgments: This work was supported by the Sapienza University of Rome—Progetto Medio di Ateneo 2020—grant no. RM120172B9361A20—"Sustainable strategies for environmental remediation and efficient use of resources".

Conflicts of Interest: The authors declare no conflict of interest.

References

1. Li, Y.; Hu, J.; Liu, H.; Zhou, C.; Tian, S. Electrochemically reversible foam enhanced flushing for PAHs-contaminated soil: Stability of surfactant foam, effects of soil factors, and surfactant reversible recovery. *Chemosphere* **2020**, *260*, 127645. [CrossRef] [PubMed]
2. Steelman, C.M.; Meyer, J.R.; Wanner, P.; Swanson, B.J.; Conway-White, O.; Parker, B.L. The importance of transects for characterizing aged organic contaminant plumes in groundwater. *J. Contam. Hydrol.* **2020**, *235*, 103728. [CrossRef] [PubMed]
3. Guo, Z.; Brusseau, M.L.; Fogg, G.E. Determining the long-term operational performance of pump and treat and the possibility of closure for a large TCE plume. *J. Hazard. Mater.* **2019**, *365*, 796–803. [CrossRef] [PubMed]
4. Huo, L.; Liu, G.; Yang, X.; Ahmad, Z.; Zhong, H. Surfactant-enhanced aquifer remediation: Mechanisms, influences, limitations and the countermeasures. *Chemosphere* **2020**, *252*, 126620. [CrossRef]
5. Liu, J.-W.; Wei, K.-H.; Xu, S.-W.; Cui, J.; Ma, J.; Xiao, X.-L.; Xi, B.-D.; He, X.-S. Surfactant-enhanced remediation of oil-contaminated soil and groundwater: A review. *Sci. Total Environ.* **2021**, *756*, 144142. [CrossRef]
6. Trellu, C.; Mousset, E.; Pechaud, Y.; Huguenot, D.; van Hullebusch, E.D.; Esposito, G.; Oturan, M.A. Removal of hydrophobic organic pollutants from soil washing/flushing solutions: A critical review. *J. Hazard. Mater.* **2016**, *306*, 149–174. [CrossRef]
7. Fu, Y.; Qin, C.; Gao, S.; Lv, C.; Zhang, C.; Yao, Y. Aquifer flushing using a SDS/1-butanol based in-situ microemulsion: Performance and mechanism for the remediation of nitrobenzene contamination. *J. Hazard. Mater.* **2022**, *424*, 127409. [CrossRef]
8. Le Meur, M.; Cohen, G.J.; Laurent, M.; Höhener, P.; Atteia, O. Effect of NAPL mixture and alteration on 222Rn partitioning coefficients: Implications for NAPL subsurface contamination quantification. *Sci. Total Environ.* **2021**, *791*, 148210. [CrossRef]
9. Liao, S.; Saleeba, Z.; Bryant, J.D.; Abriola, L.M.; Pennell, K.D. Influence of aqueous film forming foams on the solubility and mobilization of non-aqueous phase liquid contaminants in quartz sands. *Water Res.* **2021**, *195*, 116975. [CrossRef]
10. Rossi, M.; Dell'Armi, E.; Lorini, L.; Amanat, N.; Zeppilli, M.; Villano, M.; Papini, M.P. Combined strategies to prompt the biological reduction of chlorinated aliphatic hydrocarbons: New sustainable options for bioremediation application. *Bioengineering* **2021**, *8*, 109. [CrossRef]
11. Teramoto, E.H.; Pede, M.A.Z.; Chang, H.K. Impact of water table fluctuations on the seasonal effectiveness of the pump-and-treat remediation in wet–dry tropical regions. *Environ. Earth Sci.* **2020**, *79*, 435. [CrossRef]
12. Maire, J.; Joubert, A.; Kaifas, D.; Invernizzi, T.; Marduel, J.; Colombano, S.; Cazaux, D.; Marion, C.; Klein, P.-Y.; Dumestre, A.; et al. Assessment of flushing methods for the removal of heavy chlorinated compounds DNAPL in an alluvial aquifer. *Sci. Total Environ.* **2018**, *612*, 1149–1158. [CrossRef] [PubMed]
13. Ciampi, P.; Esposito, C.; Cassiani, G.; Deidda, G.P.; Rizzetto, P.; Papini, M.P. A field-scale remediation of residual light non-aqueous phase liquid (LNAPL): Chemical enhancers for pump and treat. *Environ. Sci. Pollut. Res.* **2021**, *28*, 35286–35296. [CrossRef] [PubMed]
14. Yang, C.; Offiong, N.-A.; Chen, X.; Zhang, C.; Liang, X.; Sonu, K.; Dong, J. The role of surfactants in colloidal biliquid aphrons and their transport in saturated porous medium. *Environ. Pollut.* **2020**, *265*, 114564. [CrossRef]
15. García-Cervilla, R.; Romero, A.; Santos, A.; Lorenzo, D. Surfactant-enhanced solubilization of chlorinated organic compounds contained in DNAPL from lindane waste: Effect of surfactant type and pH. *Int. J. Environ. Res. Public Health* **2020**, *17*, 4494. [CrossRef] [PubMed]
16. Alasiri, H.S.; Sultan, A.S.; Chapman, W.G. Effect of surfactant headgroup, salts, and temperature on interfacial properties: Dissipative particle dynamics and experiment for the water/octane/surfactant system. *Energy Fuels* **2019**, *33*, 6678–6688. [CrossRef]
17. Xu, Y.; Zhang, Y.; Liu, X.; Chen, H.; Fang, Y. Retrieving oil and recycling surfactant in surfactant-enhanced soil washing. *ACS Sustain. Chem. Eng.* **2018**, *6*, 4981–4986. [CrossRef]
18. Gaudin, T.; Rotureau, P.; Pezron, I.; Fayet, G. New QSPR models to predict the critical micelle concentration of sugar-based surfactants. *Ind. Eng. Chem. Res.* **2016**, *55*, 11716–11726. [CrossRef]
19. Malkapuram, S.T.; Sharma, V.; Gumfekar, S.P.; Sonawane, S.; Sonawane, S.; Boczkaj, G.; Seepana, M.M. A review on recent advances in the application of biosurfactants in wastewater treatment. *Sustain. Energy Technol. Assess.* **2021**, *48*, 101576. [CrossRef]
20. Huang, Z.; Chen, Q.; Yao, Y.; Chen, Z.; Zhou, J. Micro-bubbles enhanced removal of diesel oil from the contaminated soil in washing/flushing with surfactant and additives. *J. Environ. Manag.* **2021**, *290*, 112570. [CrossRef]
21. Babaei, M.; Copty, N.K. Numerical modelling of the impact of surfactant partitioning on surfactant-enhanced aquifer remediation. *J. Contam. Hydrol.* **2019**, *221*, 69–81. [CrossRef] [PubMed]
22. Church, J.; Willner, M.R.; Renfro, B.R.; Chen, Y.; Diaz, D.; Lee, W.H.; Dutcher, C.S.; Lundin, J.G.; Paynter, D.M. Impact of interfacial tension and critical micelle concentration on bilgewater oil separation. *J. Water Process Eng.* **2021**, *39*, 101684. [CrossRef]
23. Kłosowska-Chomiczewska, I.; Mędrzycka, K.; Hallmann, E.; Karpenko, E.; Pokynbroda, T.; Macierzanka, A.; Jungnickel, C. Rhamnolipid CMC prediction. *J. Colloid Interface Sci.* **2017**, *488*, 10–19. [CrossRef]

24. Hinton, Z.R.; Alvarez, N.J. A molecular parameter to scale the Gibbs free energies of adsorption and micellization for nonionic surfactants. *Colloids Surf. A Physicochem. Eng. Asp.* **2021**, *609*, 125622. [CrossRef]
25. Hafidi, Z.; El Achouri, M. The effect of polar head and chain length on the physicochemical properties of micellization and adsorption of amino alcohol-based surfactants. *J. Surfactants Deterg.* **2019**, *22*, 663–672. [CrossRef]
26. Gaudin, T.; Lu, H.; Fayet, G.; Berthauld-Drelich, A.; Rotureau, P.; Pourceau, G.; Wadouachi, A.; Van Hecke, E.; Nesterenko, A.; Pezron, I. Impact of the chemical structure on amphiphilic properties of sugar-based surfactants: A literature overview. *Adv. Colloid Interface Sci.* **2019**, *270*, 87–100. [CrossRef]
27. Kanokkarn, P.; Shiina, T.; Santikunaporn, M.; Chavadej, S. Equilibrium and dynamic surface tension in relation to diffusivity and foaming properties: Effects of surfactant type and structure. *Colloids Surf. A Physicochem. Eng. Asp.* **2017**, *524*, 135–142. [CrossRef]
28. Pérez, L.; Pons, R.; Oliveira de Sousa, F.F.; del Carmen Morán, M.; da Silva, A.R.; Pinazo, A. Green cationic arginine surfactants: Influence of the polar head cationic character on the self-aggregation and biological properties. *J. Mol. Liq.* **2021**, *339*, 116819. [CrossRef]
29. Cheng, M.; Zeng, G.; Huang, D.; Yang, C.; Lai, C.; Zhang, C.; Liu, Y. Advantages and challenges of Tween 80 surfactant-enhanced technologies for the remediation of soils contaminated with hydrophobic organic compounds. *Chem. Eng. J.* **2017**, *314*, 98–113. [CrossRef]
30. Befkadu, A.A.; Chen, Q. Surfactant-enhanced soil washing for removal of petroleum hydrocarbons from contaminated soils: A review. *Pedosphere* **2018**, *28*, 383–410. [CrossRef]
31. Chen, W.; Schechter, D.S. Surfactant selection for enhanced oil recovery based on surfactant molecular structure in unconventional liquid reservoirs. *J. Pet. Sci. Eng.* **2021**, *196*, 107702. [CrossRef]
32. Dominguez, C.M.; Romero, A.; Santos, A. Selective removal of chlorinated organic compounds from lindane wastes by combination of nonionic surfactant soil flushing and Fenton oxidation. *Chem. Eng. J.* **2019**, *376*, 120009. [CrossRef]
33. Jesus, C.F.; Alves, A.A.; Fiuza, S.M.; Murtinho, D.; Antunes, F.E. Mini-review: Synthetic methods for the production of cationic sugar-based surfactants. *J. Mol. Liq.* **2021**, *342*, 117389. [CrossRef]
34. Jahan, R.; Bodratti, A.M.; Tsianou, M.; Alexandridis, P. Biosurfactants, natural alternatives to synthetic surfactants: Physicochemical properties and applications. *Adv. Colloid Interface Sci.* **2020**, *275*, 102061. [CrossRef] [PubMed]
35. Madrid, F.; Ballesteros, R.; Lacorte, S.; Villaverde, J.; Morillo, E. Extraction of PAHS from an aged creosote-polluted soil by cyclodextrins and rhamnolipids. Side effects on removal and availability of potentially toxic elements. *Sci. Total Environ.* **2019**, *653*, 384–392. [CrossRef]
36. Pironti, C.; Motta, O.; Ricciardi, M.; Camin, F.; Cucciniello, R.; Proto, A. Characterization and authentication of commercial cleaning products formulated with biobased surfactants by stable carbon isotope ratio. *Talanta* **2020**, *219*, 121256. [CrossRef] [PubMed]
37. Zulkifli, N.N.; Mahmood, S.M.; Akbari, S.; Manap, A.A.A.; Kechut, N.I.; Elrais, K.A. Evaluation of new surfactants for en-hanced oil recovery applications in high-temperature reservoirs. *J. Pet. Explor. Prod. Technol.* **2020**, *10*, 283–296. [CrossRef]
38. Nguyen, T.T.; Sabatini, D.A. Characterization and emulsification properties of rhamnolipid and sophorolipid biosurfactants and their applications. *Int. J. Mol. Sci.* **2011**, *12*, 1232–1244. [CrossRef]
39. Feng, L.; Jiang, X.; Huang, Y.; Wen, D.; Fu, T.; Fu, R. Petroleum hydrocarbon-contaminated soil bioremediation assisted by isolated bacterial consortium and sophorolipid. *Environ. Pollut.* **2021**, *273*, 116476. [CrossRef]
40. Chen, Q.; Bao, M.; Fan, X.; Liang, S.; Sun, P. Rhamnolipids enhance marine oil spill bioremediation in laboratory system. *Mar. Pollut. Bull.* **2013**, *71*, 269–275. [CrossRef]
41. Bubić Pajić, N.; Ilić, T.; Nikolić, I.; Dobričić, V.; Pantelić, I.; Savić, S. Alkyl polyglucoside-based adapalene-loaded microemulsions for targeted dermal delivery: Structure, stability and comparative biopharmaceutical characterization with a conventional dosage form. *J. Drug Deliv. Sci. Technol.* **2019**, *54*, 101245. [CrossRef]
42. Marchant, R.; Banat, I.M. Biosurfactants: A sustainable replacement for chemical surfactants? *Biotechnol. Lett.* **2012**, *34*, 1597–1605. [CrossRef] [PubMed]
43. Rossi, M.; Silvani, L.; Amanat, N.; Petrangeli Papini, M. Biochar from pine wood, rice husks and iron-eupatorium shrubs for remediation applications: Surface characterization and experimental tests for trichloroethylene removal. *Materials* **2021**, *14*, 1776. [CrossRef] [PubMed]
44. Silvani, L.; di Palma, P.R.; Riccardi, C.; Eek, E.; Hale, S.E.; Viotti, P.; Petrangeli Papini, M. Use of biochar as alternative sorbent for the active capping of oil contaminated sediments. *J. Environ. Chem. Eng.* **2017**, *5*, 5241–5249. [CrossRef]
45. Drelich, J.; Fang, C.; White, C.L. Measurement of interfacial tension in fluid-fluid systems. *Encycl. Surf. Colloid Sci.* **2002**, *3*, 3152–3166.
46. Pal, N.; Samanta, K.; Mandal, A. A novel family of non-ionic Gemini surfactants derived from sunflower oil: Synthesis, characterization and physicochemical evaluation. *J. Mol. Liq.* **2018**, *275*, 638–653. [CrossRef]
47. Bagheri, A.; Bagheri, A. Interfacial and micellization properties of pure surfactants with similar hydrocarbon chain length (C 16 H 33) and different polar head in aqueous medium. *J. Appl. Chem.* **2021**, *15*, 55–64.
48. Rossi, M.M.; Matturro, B.; Amanat, N.; Rossetti, S.; Papini, M.P. Coupled adsorption and biodegradation of trichloroethylene on biochar from pine wood wastes: A combined approach for a sustainable bioremediation strategy. *Microorganisms* **2022**, *10*, 101. [CrossRef]

49. Silvani, L.; Vrchotova, B.; Kastanek, P.; Demnerova, K.; Pettiti, I.; Papini, M.P. Characterizing biochar as alternative sorbent for oil spill remediation. *Sci. Rep.* **2017**, *7*, srep43912. [CrossRef]
50. Amanat, N.; Matturro, B.; Villano, M.; Lorini, L.; Rossi, M.M.; Zeppilli, M.; Rossetti, S.; Petrangeli Papini, M. Enhancing the biological reductive dechlorination of trichloroethylene with PHA from mixed microbial cultures (MMC). *J. Environ. Chem. Eng.* **2022**, *10*, 107047. [CrossRef]
51. Jiménez-Peñalver, P.; Koh, A.; Gross, R.; Gea, T.; Font, X. Biosurfactants from waste: Structures and interfacial properties of sophorolipids produced from a residual oil cake. *J. Surfactants Deterg.* **2020**, *23*, 481–486. [CrossRef]
52. Rosen, M.J.; Kunjappu, J.T. *Surfactants and Interfacial Phenomena*, 4th ed.; John Wiley and Sons: Hoboken, NJ, USA, 2012.
53. Gaudin, T.; Rotureau, P.; Pezron, I.; Fayet, G. Estimating the adsorption efficiency of sugar-based surfactants from QSPR models. *Int. J. Quant. Struct. Relatsh.* **2019**, *4*, 28–51. [CrossRef]
54. Penfold, J.; Thomas, R.K.; Shen, H.-H. Adsorption and self-assembly of biosurfactants studied by neutron reflectivity and small angle neutron scattering: Glycolipids, lipopeptides and proteins. *Soft Matter* **2011**, *8*, 578–591. [CrossRef]
55. Mańko, D.; Zdziennicka, A.; Jańczuk, B. Thermodynamic properties of rhamnolipid micellization and adsorption. *Colloids Surf. B Biointerfaces* **2014**, *119*, 22–29. [CrossRef]
56. Chen, M.L.; Penfold, J.; Thomas, R.K.; Smyth, T.J.P.; Perfumo, A.; Marchant, R.; Banat, I.M.; Stevenson, P.; Parry, A.; Tucker, I.; et al. Solution self-assembly and adsorption at the air−water interface of the monorhamnose and dirhamnose rhamnolipids and their mixtures. *Langmuir* **2010**, *26*, 18281–18292. [CrossRef]
57. Li, G.; Yi, X.; Jiang, J.; Zhang, Y.; Li, Y. Dynamic surface properties and dilational rheology of acidic and lactonic sophorolipids at the air-water interface. *Colloids Surf. B Biointerfaces* **2020**, *195*, 111248. [CrossRef]
58. Martínez-Balbuena, L.; Arteaga-Jiménez, A.; Hernández-Zapata, E.; Márquez-Beltrán, C. Applicability of the Gibbs adsorption isotherm to the analysis of experimental surface-tension data for ionic and nonionic surfactants. *Adv. Colloid Interface Sci.* **2017**, *247*, 178–184. [CrossRef]
59. Wang, Z.W.; Huang, D.Y.; Li, G.Z.; Zhang, X.Y.; Liao, L.L. Effectiveness of surface tension reduction by anionic surfactants—Quantitative structure–property relationships. *J. Dispers. Sci. Technol.* **2007**, *24*, 653–658. [CrossRef]
60. Chen, W.; Wei, R.; Ni, J.; Yang, L.; Qian, W.; Yang, Y. Sorption of chlorinated hydrocarbons to biochars in aqueous environment: Effects of the amorphous carbon structure of biochars and the molecular properties of adsorbates. *Chemosphere* **2018**, *210*, 753–761. [CrossRef]
61. Schreiter, I.J.; Schmidt, W.; Schüth, C. Sorption mechanisms of chlorinated hydrocarbons on biochar produced from different feedstocks: Conclusions from single- and bi-solute experiments. *Chemosphere* **2018**, *203*, 34–43. [CrossRef]
62. Ballesteros-Gómez, A.; Rubio, S. Hemimicelles of alkyl carboxylates chemisorbed onto magnetic nanoparticles: Study and application to the extraction of carcinogenic polycyclic aromatic hydrocarbons in environmental water samples. *Anal. Chem.* **2009**, *81*, 9012–9020. [CrossRef] [PubMed]
63. Zeng, Z.; Liu, Y.; Zhong, H.; Xiao, R.; Zeng, G.; Liu, Z.; Cheng, M.; Lai, C.; Zhang, C.; Liu, G.; et al. Mechanisms for rhamnolipids-mediated biodegradation of hydrophobic organic compounds. *Sci. Total Environ.* **2018**, *634*, 1–11. [CrossRef] [PubMed]
64. Guo, Y.-P.; Hu, Y.-Y.; Lin, H.; Ou, X.-L. Sorption and desorption of 17α-ethinylestradiol onto sediments affected by rhamnolipidic biosurfactants. *J. Hazard. Mater.* **2018**, *344*, 707–715. [CrossRef] [PubMed]